

Steady-state distributions of nonequilibrium carriers in metals

O. F. Panchenko and V. M. Shatalov

Physicotechnical Institute, Academy of Sciences of the Ukrainian SSR, Donetsk

(Submitted 25 July 1986)

Zh. Eksp. Teor. Fiz. **93**, 222–230 (July 1987)

The steady-state distribution function of the energies of nonequilibrium electrons and holes formed as a result of a cascade of electron-electron collisions in the presence of a primary electron flux is found by solving the linearized transport equation in the isotropic scattering approximation. The distributions obtained in this way include dependences on the energy of primary electrons and on the characteristics of the medium. Near the Fermi level they have a singularity and are close to a power law far from this level. A study is made of the possibility of deriving distributions for crystals with a complex energy band structure.

1. INTRODUCTION

Theoretical models of steady-state distributions of nonequilibrium electrons have been developed primarily for the interpretation of the experimental results on secondary electron emission (SEE). Back in 1923 P. L. Kapitza proposed a thermal mechanism of SEE¹ which describes well the integrated characteristics, such as the dependences of the SEE current on the primary electron energy, but gives contradictory results in the interpretation of the differential spectra.² In 1954 P. A. Wolff³ solved a linearized transport equation in the isotropic scattering approximation using a model function representing energy losses and found that the spectral density of the number of secondary electrons obeys the law $N_e(E) \propto E^2$. This result has been used, for example, to reveal the fine structure of the SEE spectrum.⁴ It was shown in Ref. 5 that distributions of the $N_e(E) \propto E^s$ type are steady-state in the case of classical particles when external fluxes are present. The power exponent s is determined by the nature of the cross section, for example, in the case of the screened Coulomb interaction we have $s = -5/4$. The power-law dependence $N_e(E)$ is used in surface Auger spectroscopy⁶ to subtract the background and to identify the spectral line of an SEE source. Special experiments⁷ designed to test the power-law spectral distribution of secondary electrons emitted as a result of irradiation of a crystal with α particles demonstrated that the power exponent s is generally energy-dependent varying, for example, in the case of aluminum from -3.5 to -1.92 when the energy E is increased from 10 to 40 eV. Moreover, the limits of variation of s are different for different metals. These observations do not fit the existing models of $N_e(E)$.

A steady-state distribution of the energies of secondary electrons in a crystal should obviously depend on the primary electron energy E_p and also on the characteristics of the medium in which the scattering takes place. Such a distribution should be universal because the method of excitation of primary electrons is of no significance. For example, in the case of photoelectron emission when the depth of absorption of light is much greater than the mean free path of photoelectrons, the combined spectrum including an allowance for the scattering can be described by a convolution of $N_e(E)$ in respect of the parameter E_p with the probability of photon absorption on excitation of an electron to a level E_p . The spectrum of bremsstrahlung isochromats is a

convolution in E with the probability of photon emission due to relaxation of an electron from a level E . Interpretation of the radiative recombination spectra of nonequilibrium electrons (electron-photon emission)⁸ also depends strongly on the form of $N_e(E)$. The energy of a level E from which a radiative transition originates may be higher or lower than the energy E_F of the Fermi level. In the latter case it is necessary to know the distribution of nonequilibrium holes $N_h(E)$.

Our aim will be to determine the steady-state distribution function of the energies of nonequilibrium carriers when the primary (excitation) energies E_p do not exceed the plasma energy $E_F + \hbar\omega_{pl}$, so that this function should satisfy as much as possible the above requirements. The first step in this direction was made by one of the present authors in Ref. 9 where, as in Ref. 3, a solution was obtained of the steady-state transport equation, but the rate of energy losses and the average electron lifetime $\tau(E)$ were calculated using a theory of an interacting electron gas.¹⁰ The following approximate analytic solution was obtained for the case when $E_p < E_F + \hbar\omega_{pl}$:

$$\frac{N_e(E)}{N_p} = \frac{4}{(E_p - E_F) 17^{1/2}} \left[\left(\frac{E_p - E_F}{E - E_F} \right)^{(17^{1/2} + 3)/2} - \left(\frac{E - E_F}{E_p - E_F} \right)^{(17^{1/2} - 3)/2} \right], \quad (1)$$

where N_p is the concentration of primary electrons. In the present paper our task will be to obtain simultaneously the distributions of nonequilibrium electrons and holes using the relevant equations formulated in Sec. 2; we shall also study the possibility of modeling the energy loss function for real crystals in Sec. 3 and give numerical analytic solutions for the investigated models in Sec. 4. The results will be discussed in Sec. 5.

2. SYSTEM OF EQUATIONS FOR THE DISTRIBUTION FUNCTIONS OF NONEQUILIBRIUM ELECTRONS AND HOLES

The steady-state condition for a distribution function $f(E)$ dependent only on the energy specifies that the collision integral should vanish in the range $E < E_p$. This integral can be linearized because in the case of the problems under discussion we find that the condition $f(E) \gg 1$ is satisfied well when $E > E_F + \varepsilon$ and the condition $1 - f(E) \ll 1$ is

obeyed when $E < E_F - \varepsilon$; here, ε is a small region near E_F where these conditions are not met. In fact, the range of energies of nonequilibrium carriers encountered in the experiments described above never overlaps this region. For convenience, we shall not speak of the distribution functions but of the energy densities of the concentrations of nonequilibrium electrons and holes:

$$N_e(E) = f(E)\rho(E), \quad E > E_F, \quad (2)$$

$$N_h(E) = [1 - f(E)]\rho(E), \quad E < E_F,$$

where $\rho(E)$ is the density of states. We shall discuss the range of energies where the electron-electron scattering predominates, at least in metals. Such scattering of excited electrons creates a certain concentration $N_h(E)$ of nonequilibrium holes which in turn are scattered giving rise to nonequilibrium electrons. The excitation energy of the latter is limited by the maximum excitation energy of holes.

We have therefore two coupled subsystems of electrons and holes for which the steady-state condition gives the following system of equations:

$$\int_{\varepsilon}^{E_p} S_{ee}(E', E) N_e(E') dE' + \int_{\max(0, 2E_F - E_p)}^{2E_F - E} S_{he}(E', E) N_h(E') dE' - \Gamma_e(E) N_e(E) + I_p \delta(E - E_p) = 0, \quad E > E_F + \varepsilon, \quad (3)$$

$$\int_{\max(0, 2E_F - E_p)}^E S_{hh}(E', E) N_h(E') dE' + \int_{2E_F - E}^{E_p} S_{eh}(E', E) N_e(E') dE' - \Gamma_h(E) N_h(E) = 0, \quad E < E_F - \varepsilon.$$

The system of equations (3) denotes equality of the number of particles arriving at a level E and leaving this level E per unit time; $S_{ee}(E', E)$ is the rate of arrival of electrons at the level E because of the scattering of electrons by a level E' ; $S_{he}(E', E)$ describes the rate of arrival of electrons at the level E because of the scattering of holes by the level E' ; S_{hh} and S_{eh} are defined in a similar manner; $\Gamma_e(E)$ and $\Gamma_h(E)$ are the total rates of relaxation or the reciprocal lifetimes of electrons and holes; the last term in the first equation of the system (3) is the source function; I_p is the number of primary electrons generated per unit time in a unit volume. The limits of integration in the system (3) obviously represent the regions of definition of the quantities occurring here and the energies should be measured from the bottom of the conduction band.

In the case of relative relaxation fluxes of the scattered particles

$$\Phi_e(E) = N_e(E)\Gamma_e(E)/I_p - \delta(E - E_p), \quad E > E_F, \quad (4)$$

$$\Phi_h(E) = N_h(E)\Gamma_h(E)/I_p, \quad E < E_F$$

we obtain from the system (3) the following system of integral equations

$$\begin{aligned} \Phi_e(E) &= \int_{\varepsilon}^{E_p} P_{ee}(E', E) \Phi_e(E') dE' \\ &+ \int_{\max(0, 2E_F - E_p)}^{2E_F - E} P_{he}(E', E) \Phi_h(E') dE' \\ &+ P_{ee}(E_p, E), \quad E_F + \varepsilon < E < E_p, \end{aligned} \quad (5)$$

$$\begin{aligned} \Phi_h(E) &= \int_{\max(0, 2E_F - E_p)}^E P_{hh}(E', E) \Phi_h(E') dE' \\ &+ \int_{2E_F - E}^{E_p} P_{eh}(E', E) \Phi_e(E') dE' \\ &+ P_{eh}(E_p, E), \quad 0 < E < E_F - \varepsilon, \end{aligned}$$

where

$$P_{\alpha\beta}(E_1, E_2) = S_{\alpha\beta}(E_1, E_2)/\Gamma_{\alpha}(E_1), \quad \alpha, \beta = e, h. \quad (6)$$

The quantity defined by Eq. (6) represents the fraction of particles which decay in the $E_1 \rightarrow E_2$ channel.

The following important properties of the system (5) and of the quantities occurring there should be noted.

1. If $E \geq 2E_F$, the second term in the first equation of the system (5) disappears and the electron energy distribution becomes independent of the hole energy distribution. This problem was considered in Ref. 9.

2. Solutions of the systems $\Phi_e(E)$ and $\Phi_h(E)$ depend only on the partial fractions of the scattering characterized by a specific energy loss for each level $P_{\alpha\beta}(E_1, E_2)$ and are independent of the absolute values of the rates of relaxation $S_{\alpha\beta}(E_1, E_2)$ and $\Gamma_{\alpha}(E_1)$, where $\alpha, \beta = e, h$. Consequently, in the search for the solution we can use the scattering rates determined only to within an arbitrary factor $\xi(E_1)$.

3. The quantities P_{ee} , P_{hh} and P_{eh} , P_{he} are normalized differently:

$$\int P_{ee}(E, E') dE' = \int P_{hh}(E, E') dE' = 2, \quad (7)$$

$$\int P_{eh}(E, E') dE' = \int P_{he}(E, E') dE' = 1. \quad (8)$$

This occurs because when electrons are scattered we obtain two excited electrons and only one hole in the final state, whereas the scattering of a hole creates two holes and one excited electron. This difference between the normalizations gives rise to an asymmetry of the boundary conditions for the system (5) and, as shown later, in some cases it causes divergence of the quantity representing the total charge of a sample:

$$\int_0^{E_F - \varepsilon} N_h(E) dE - \int_{E_F + \varepsilon}^{E_p} N_e(E) dE \quad \text{for } \varepsilon \rightarrow 0.$$

These problems will be discussed in greater detail in the next section.

3. MODELING OF SCATTERING RATES

The total scattering rate is determined by the imaginary part of the self-energy correction to the energy¹⁰: $\text{Im}\Sigma(E) = \hbar\Gamma(E)/2$; the indices e and h introduced by us simply identify a specific range of E . We are considering here a quantity averaged over the directions of the wave vector \mathbf{k} . The quantity $\Gamma_e(E_1)$ can be defined, for example, as the probability of the scattering (per unit time) of an electron at a level E_1 , summed over all the final states of the scattering products which are electrons at levels E_2 and E_3 and a hole at a level E_4 :

$$\begin{aligned} \Gamma_e(E_1) &= \frac{1}{2} \int \rho(E_2) dE_2 \int \rho(E_3) dE_3 \int \rho(E_4) dE_4 \\ &\cdot w(E_2, E_3; E_1, E_1) \delta(E_1 + E_4 - E_2 - E_3). \end{aligned} \quad (9)$$

The factor 1/2 appears because of the identity of electrons at the levels E_2 and E_3 and, consequently, because of indistinguishability of the states which differ by their transposition. In this respect our treatment differs from a theory developed for classical particles in Ref. 5.

The partial scattering rates are then defined as follows:

$$S_{ee}(E_1, E_2) = \rho(E_2) \int \rho(E_3) dE_3 \int \rho(E_4) dE_4 \cdot w(E_2, E_3; E_4, E_1) \delta(E_1 + E_4 - E_2 - E_3), \quad (10)$$

$$S_{eh}(E_1, E_4) = \frac{1}{2} \rho(E_4) \int \rho(E_2) dE_2 \int \rho(E_3) dE_3 \cdot w(E_2, E_3; E_4, E_1) \delta(E_1 + E_4 - E_2 - E_3). \quad (11)$$

Integrating ratios representing division of Eqs. (10) and (11) by Eq. (9), we obtain the normalizations (7) and (8), respectively.

The coefficient $w(E_2, E_3; E_4, E_1)$ in front of the δ function in Eqs. (9)–(11) represents the square of the matrix element of the scattering process averaged over the directions of the wave vector \mathbf{k}_1 . If we assume that it is independent of the energy, we obtain the familiar Berglund-Spicer approximation¹¹ in which the scattering rates are found allowing solely for the statistical weight of the final states. Moreover, as shown above, we can solve the system (5) by assuming that this coefficient is a function of $\xi(E_1)E_F$. Therefore, in the Berglund-Spicer approximation the singularities of the real dispersion law of carriers are reflected in the scattering probabilities given by Eqs. (9)–(11) via the density of states $\rho(E)$.

We can solve the system (5) analytically by assuming that $\rho(E) = \text{const}/E_F$ if $\rho(E) \neq 0$. It then follows from the law of conservation of energy that in the range $E_p \leq 2E_F$ we have

$$\begin{aligned} S_{ee}(E_1, E_2) &= -S_{hh}(E_1, E_2) = \xi(E_1) (E_1 - E_2) / E_F^2, \\ S_{eh}(E_1, E_2) &= -S_{he}(E_1, E_2) = \xi(E_1) (E_1 + E_2 - 2E_F) / 2E_F^2, \\ \Gamma_e(E_1) &= \Gamma_h(E_1) = \xi(E_1) (E_1 - E_F)^2 / 4E_F^2. \end{aligned} \quad (12)$$

Before we solve the system (5) in any one of these approximations, we shall check whether these approximations are satisfactory by considering the jellium model in which the energy loss function $S(E_1, E_2)$ and the reciprocal of the elec-

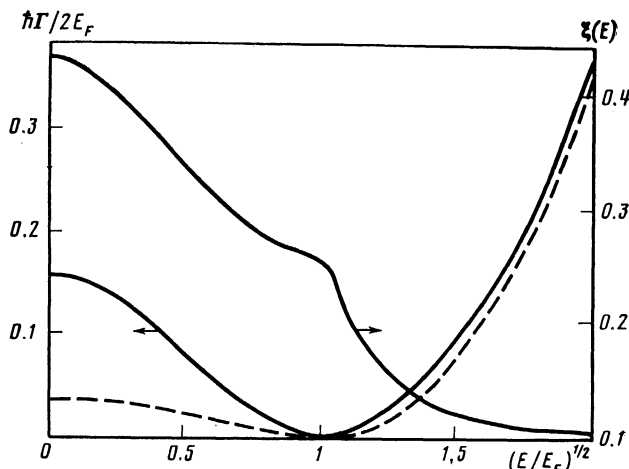


FIG. 1. Rate of electron-electron scattering or the reciprocal lifetime $\Gamma(E)$ in the jellium model⁹ (continuous curve) and in the Berglund-Spicer approximation¹² for a quadratic dispersion law (dashed curve). The ratio of the two curves $\xi(E)$ represents the average value of the square of the scattering matrix element (continuous curve).

tron lifetime $\Gamma(E_1)$ can be calculated relatively rigorously⁹ using the theory of an interacting electron gas.¹⁰ Figure 1 compares $\Gamma(E)$ obtained using the jellium model and that found employing the Berglund-Spicer approximation in the case of the quadratic dispersion law $E = p^2/2m$. The ratio of these quantities provides a definition of the unknown coefficient $\xi(E)$ (Fig. 1), by which we have to divide the solution of Eq. (5), in accordance with the definition of Eq. (4), in order to go over to $N(E)$. The loss functions for electrons and holes obtained using this factor for different initial energies are compared in Fig. 2 with the results obtained on the basis of the jellium model. We can see that the Berglund-Spicer approximation, which is fully satisfactory at low transferred energies, becomes less acceptable in the case of high losses. Nevertheless, the curves representing the distributions of nonequilibrium electrons remains similar and very close for all three models when the excitation energy is increased up to $E_p = 4E_F$ (Fig. 3). The $N_e(E)$ curve obtained in the jellium model and in the Berglund-Spicer approximation are the results of a numerical solution of the system (5) obtained ignoring the influence of the hole distribution. The corresponding analytic form of Eq. (1) was obtained in Ref. 9 using the approximation of Eq. (12). The distributions plotted in Fig. 3 are examples of a successful application of the Berglund-Spicer approximation and of the approximation defined by Eq. (12), so that one would hope to obtain satisfactory results by analytic solution of the system (5) in the case of small values of E_p and using the Berglund-Spicer approximation in the case of crystals with a complex energy band structure, possibly semiconductors and insulators, in other words, using this approximation in those cases when the jellium model is unacceptable.

4. SOLUTION OF THE SYSTEM OF TRANSPORT EQUATIONS

We shall now give the results of numerical (in the Berglund-Spicer approximation) and analytic [in the model of Eq. (12)] solutions of the system of equations (5). In both cases we have to deal separately with the ranges $E_p \leq 2E_F$ and $E_p > 2E_F$.

If $E_p \leq 2E_F$, the distributions of nonequilibrium holes and electrons differ from zero in the intervals $(2E_F - E_p, E_F)$ and (E_F, E_p) , respectively. For all values of

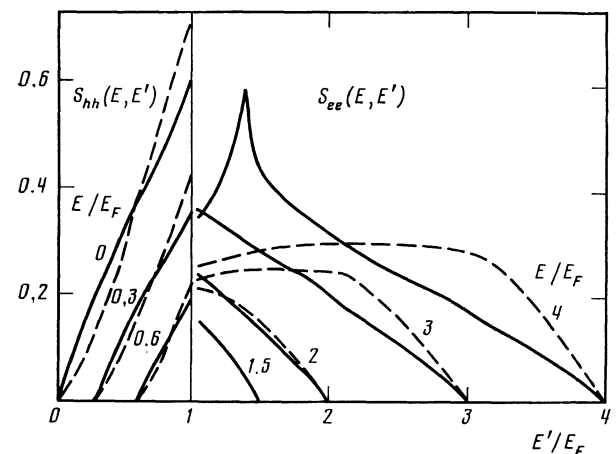


FIG. 2. Rates of energy losses experienced by electrons and holes (in units of E_F/\hbar), calculated for different initial energies given alongside the curves: the continuous curves represent the jellium model and the dashed curves represent the Berglund-Spicer approximation.

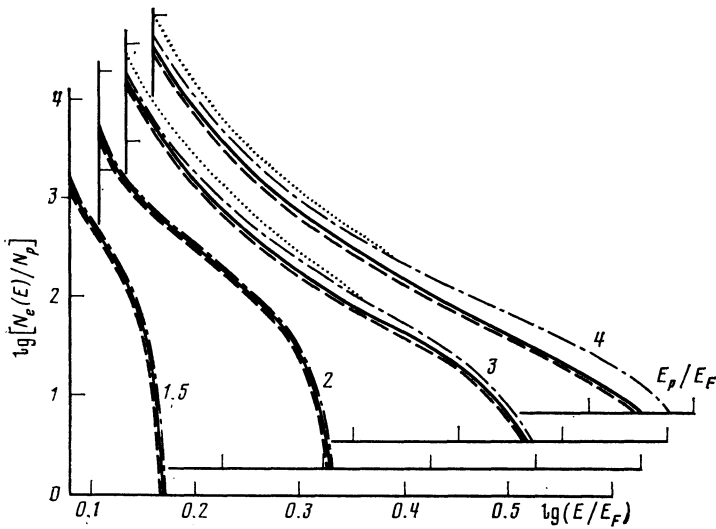


FIG. 3. Steady-state distributions of nonequilibrium electrons obtained for different primary electron energies, given alongside the curves. The continuous curves represent the jellium model, the dashed curves correspond to Eq. (1), and the chain curves represent the Berglund-Spicer approximation. The dotted curves show the changes due to an allowance for the scattering of holes.

If the equations in the system (5) are coupled. Using the scattering probability in the form of Eq. (12), we can obtain an analytic solution by reducing a system of two integral equations to one fourth-order differential equation. Allowing for the initial conditions, we obtain

$$N_e(E) = A_p(E) (3/5x^4 + 1/3x^3 - 1/3 - 3x/5), \quad 0 < x < 1, \quad (13)$$

$$N_h(E) = A_p(E) (3/5x^4 + 1/3x^3 + 1/3 + 3x/5), \quad -1 < x < 0,$$

where

$$A_p(E) = N_p \xi(E_p) / (E_p - E_F) \xi(E),$$

$N_p = I_p / \Gamma(E_p)$ is the concentration of primary electrons, and $x = (E - E_F) / (E_p - E_F)$ is a dimensionless energy parameter. The solution represented by the system (13) does not exhibit a definite parity in respect of x , which—as mentioned above—is associated with the asymmetry of the

boundary conditions for $\Phi_e(E)$ and $\Phi_h(E)$.

If $E_p > 2E_F$, there is an interval $(2E_F, E_p)$ in which $N_e(E)$ is defined without influence of the hole distribution. The model of Eq. (12) gives the distribution in the form of Eq. (1), which can be used to obtain the boundary conditions for the system (5). However, we cannot solve the system analytically using this model. An analytic solution can be obtained in the range $E_1 > 2E_F$ by supplementing the model of Eq. (12) with a model similar to that suggested in Ref. 9:

$$\begin{aligned} S_{ee}(E_1, E_2) &= \xi(E_1) / 2(E_1 - E_F), & S_{eh}(E_1, E_2) &= \xi(E_1) / 4E_F, \\ \Gamma_e(E_1) &= \xi(E_1) / 4. \end{aligned} \quad (14)$$

When the system (5) is supplemented in this way, it can be solved analytically and we then obtain

$$\begin{aligned} N_e(E) &= B_p(E) \begin{cases} \left[\left(\frac{1}{z^4} + \frac{2z}{3} \right) \left(\frac{6E_p}{5E_F} - \frac{3}{2} \right) + \frac{1}{3z^3} + \frac{1}{6z} \right], & 0 < z < 1 \\ \frac{2}{z^2} \left(\frac{E_p}{E_F} - 1 \right), & 1 < z < \frac{E_p}{E_F} - 1 \end{cases}, \\ N_h(E) &= B_p(E) \left[\left(\frac{1}{z^4} - \frac{2z}{3} \right) \left(\frac{6E_p}{5E_F} - \frac{3}{2} \right) + \frac{1}{3z^3} - \frac{1}{6z} \right], & -1 < z < 0, \end{aligned} \quad (15)$$

where $B_p(E) = N_p \xi(E_p) / E_F \xi(E)$, and $z = E / E_F - 1$ is an energy parameter.

A numerical solution of the system (9) using the scattering probabilities in the Berglund-Spicer approximation presents no difficulties because it is possible to derive an algorithm such that when the energy E is scanned from E to $E_F + \varepsilon$ each successive value of $N_e(E)$ and $N_h(2E_F - E)$ is defined in a recurrent manner in terms of the values already found. The results of such a calculation carried out on the assumption of the quadratic dispersion law are plotted in Fig. 4 for $E_p = 4E_F$. The shaded region demonstrates the changes in $N_e(E)$ introduced by including the scattering of holes; the same differences are represented by dashed curves

in Fig. 3. The contribution made by the scattering of holes to $N_e(E)$ tends to zero as E increases to $2E_F$. Figure 4 shows also the energy distribution curve for the SEE current $j(E)$ which is obtained if $N_e(E)$ is multiplied by the electron velocity $v = (2E/m)^{1/2}$ and by the coefficient representing the transmission of the crystal-vacuum barrier:

$$\kappa(E) = 1 - [(E_p + e\varphi) / E]^{1/2}, \quad E > E_p + e\varphi,$$

where $e\varphi$ is the work function assumed to be $0.3E_F$. The spectrum of the SEE current has a characteristic cascade maximum. We can determine the influence of the excitation conditions on the position and profile of this maximum by calculating similarly the value of $j(E)$ for different primary

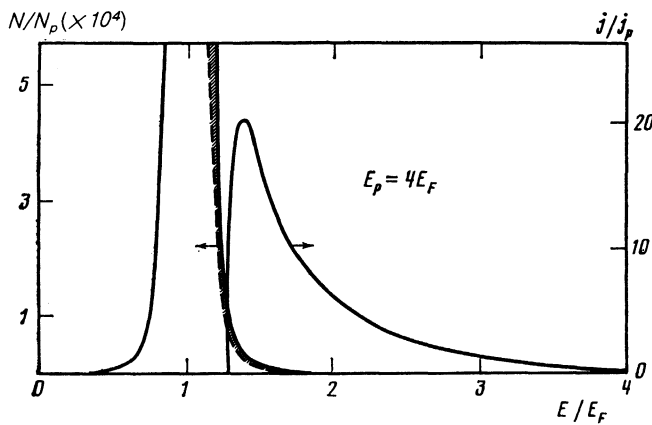


FIG. 4. Steady-state distributions of nonequilibrium electrons and holes obtained by solving the system (5) in the Berglund-Spicer approximation when $E_p = 4E_F$ (left-hand scale). The shaded region is the contribution made by the scattering of holes. The right-hand scale represents the cascade distribution of the secondary electron emission current.

electron energies E_p (Fig. 5). We can see that at least at low values of E_p the form of the $j(E)$ curves varies considerably on increase in E_p and the position of the cascade maximum then shifts somewhat toward higher energies. Therefore, the specific excitation conditions should be allowed for in the interpretation of the experimental curves.

5. DISCUSSION OF RESULTS

We thus have an algorithm for the calculation of steady-state distributions of nonequilibrium electrons and holes in crystals with a complex dispersion law and we know the analytic forms of the dependences $N_e(E)$ and $N_h(E)$ for simple metals in the range of energies where the electron-plasmon scattering is unimportant. A partial analysis of the assumed approximations can be found in Refs. 3, 5, and 11. Here, we shall simply mention our result which is a slow change in the average value of the square of the scattering matrix element $\xi(E)$ in the most interesting range $E > E_F + \varepsilon$ (Fig. 1) and the fact that the final result depends only multiplicatively on $\xi(E)$.

All the models discussed by us predict an unbounded rise of $N_e(E)$ and $N_h(E)$ in the limit $E_p \rightarrow E_F$, which is fun-

damentally different from the power-law distributions obtained in Refs. 3 and 5, where the region of degeneracy of the electron gas was ignored and the particles were regarded as classical. Our results are fully justified physically because an infinite number of changes of the energy of an excited electron should create an infinite number of electron-hole pairs near the Fermi level. In fact, when this number is compared with the concentration of equilibrium electrons, the Pauli principle holds and our analysis is no longer correct. This is the reason for the limitation $|E - E_F| > \varepsilon$ introduced above. In the intermediate range $E_F \ll E \ll E_p$ our distribution is close to a power law (Fig. 3) and the power exponent is the slope and increases on reduction in the energy, in qualitative agreement with the experimental results.⁷ Our aim was not to carry out a detailed comparison with the experimental results because this would require the knowledge of the actual conditions of excitation of primary electrons. The difference between the excitation conditions may be responsible for the difference between the SEE spectra obtained on irradiation of a crystal with α particles and with fission fragments.²

The proposed procedure gives the absolute values of SEE yield without any fitting parameters and this makes it possible to calculate simultaneously the primary spectra. The analytic results obtained above can be used directly in calculations of the spectra of bremsstrahlung isochromats and of photoelectron spectra allowing for the scattering processes at photon energies right up to vacuum ultraviolet.

Extension of the algorithm to higher values of E_p requires an allowance for the electron-plasmon scattering, as suggested in Ref. 9, or introduction of fitting parameters in Eq. (14) to make these distributions useful, for example, in calculations of the electron-photon emission spectra. Since the distribution obtained above is universal, these parameters can be used in various experiments.

The authors are deeply grateful to K.B. Tolpygo for valuable discussions and comments.

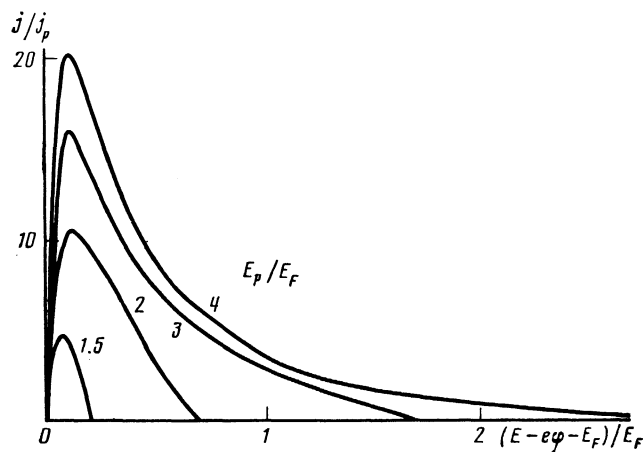


FIG. 5. Distribution of the secondary electron emission current obtained for different values of the primary electron energy given alongside the curves. The values along the ordinates in Figs. 4 and 5 are in units of E_F .

¹P. L. Kapitza, *Philos. Mag.* **45**, 989 (1923).

²V. M. Agranovich, D. K. Daukeev, Yu. V. Konobeev, and S. Ya. Lebedev, *Zh. Eksp. Teor. Fiz.* **57**, 401 (1969) [*Sov. Phys. JETP* **30**, 220 (1970)].

³P. A. Wolff, *Phys. Rev.* **95**, 56 (1954).

⁴O. M. Artamonov, O. M. Smirnov, and A. N. Terekhov, *Izv. Akad. Nauk Ser. Fiz.* **46**, 1383 (1982).

⁵V. I. Karas', S. S. Moiseev, and V. E. Novikov, *Zh. Eksp. Teor. Fiz.* **71**, 1421 (1976) [*Sov. Phys. JETP* **44**, 744 (1976)].

⁶E. N. Sickafus, *Phys. Rev. B* **16**, 1436, 1448 (1977).

⁷E. N. Batrakin, I. I. Zalyubovskii, V. I. Karas', S. I. Kononenko, V. N. Mel'nik, S. S. Moiseev, and V. I. Muratov, *Zh. Eksp. Teor. Fiz.* **89**, 1098 (1985) [*Sov. Phys. JETP* **62**, 633 (1985)].

⁸Yu. A. Kulyupin, A. F. Fedosenko, V. M. Shatalov, and A. I. Shchurenko, *Pis'ma Zh. Eksp. Teor. Fiz.* **40**, 298 (1984) [*JETP Lett.* **40**, 1086 (1984)].

⁹V. M. Shatalov, *Solid State Commun.* **59**, 53 (1986).

¹⁰D. Pines, *Elementary Excitations in Solids*, Benjamin, New York (1963).

¹¹C. N. Berglund and W. E. Spicer, *Phys. Rev. A* **136**, 1030 (1964).

Translated by A. Tybulewicz